BBA - General Subjects 1863 (2019) 1235–1242

Contents lists available at ScienceDirect

BBA - General Subjects

journal homepage: www.elsevier.com/locate/bbagen

Application of digital PCR for assessing DNA fragmentation in cytotoxicity response

Jeongran Han[a,b], Ji Youn Lee[a], Young-Kyung Bae[a,*]

[a] Center for Bioanalysis, Korea Research Institute of Standards and Science, 267 Gajeong-ro, Yuseong-gu, Daejeon, Republic of Korea
[b] Department of Biological Sciences, Korea Advanced Institute of Science and Technology, 291 Daehak-ro, Yuseong-gu, Daejeon, Republic of Korea

ARTICLE INFO

Keywords:
DNA fragmentation
Digital PCR
Cytotoxicity
Regulated cell death

ABSTRACT

Background: Regulated cell death plays an essential role in various biological processes, leading to the development of a number of methods to detect and quantitatively measure cells exhibiting decreased viability due to either apoptosis or necrosis.
Methods and results: When cytotoxicity is induced by anti-cancer chemicals, human cell lines exhibit specific features, including dampened cell proliferation and lost plasma membrane asymmetry, presenting distinct sensitivity. In this study, we report a set of novel digital PCR (dPCR) assays to quantitatively measure the degree of cell death. These dPCR assays are designed to quantify targets of increasing sizes within the RNase P (RP) gene locus. The ratio between short and long target copy numbers implies the degree of DNA fragmentation, which we name the *RP fragmentation index*.
Conclusions: Compared to other conventional quantitative methods, the RP fragmentation index using cellular DNA represents a valid indicator in the measurement of the degree of cell death.
General significance: The demonstrated dPCR assays can precisely assess DNA fragmentation that quantitatively reflects the degree of cytotoxicity.

1. Introduction

Assessment of regulated cell death is crucial as it plays essential roles in various cellular-related areas including development, cancer progression, and immune response [1,2]. While the process of regulated cell death can be elicited either with or without external perturbations, both result in similar macromolecular and biochemical changes [1]. Major characteristics of cells undergoing cell death include shrinkage of their plasma membrane, formation of apoptotic bodies, DNA fragmentation via nuclear disruptions, and activation of caspases and endonucleases [3]. These distinct features are targets in various techniques for detecting and quantifying cell death, making them critical in new cancer drug testing or measurements of cytotoxicity under environmentally perturbed conditions. As a result, there has been great interest and wide efforts to develop sensitive and reliable methods for detecting and quantifying levels of cell death.

DNA fragmentation is a specific marker for apoptosis [4]. Numerous techniques for identifying and measuring DNA fragmentation have been developed as a means of detecting cell death, including the DNA ladder assay, comet assay, and terminal deoxynucleotidyl transferase deoxynucleotide (dUTP) nick end labeling (TUNEL) assay. In the DNA ladder assay, isolated cellular DNA from lysed cells are separated and visualized on agarose gel [3]. DNA from apoptotic cells exhibits a “ladder” pattern on a gel, presenting a characteristic internucleosomal cleavage. The comet assay employs a similar approach in which DNA breaks are visualized at the single-cell level; fragmented DNA separates from intact genomic DNA in the nuclear core, which can be measured by image analysis. On the other hand, the TUNEL assay takes advantage of terminal deoxynucleotidyl transferase (TdT) endonuclease activity that attaches a modified dUTP to DNA strand breaks. Such dUTP analogues can appear either as a fluorescently labeled form or as bromodeoxyuridine (BrdU). For each of the aforementioned methods to succeed with sufficient sensitivity, multiple requirements must first be met [3]. Consequently, a set of independent principles with which to compare the results obtained by such various methods has become a necessity.

Patterns of DNA fragmentation resulting from cell death can also be identified in plasma cell-free DNA (cfDNA) [5,6], which has drawn increasing interest in various fields including cancer diagnosis [7,8]. Although the detection of cancer-specific mutations is the primary aim for circulating tumor DNA (ctDNA) analyses, the levels of integrity and fragmentation of circulating cfDNA has also been explored [9–13]. Estimations of ctDNA fragmentation levels have adopted quantitative

* Corresponding author.
E-mail address: ybae@kriss.re.kr (Y.-K. Bae).

https://doi.org/10.1016/j.bbagen.2019.05.001
Received 8 January 2019; Received in revised form 4 April 2019; Accepted 2 May 2019
Available online 07 May 2019

polymerase chain reaction (qPCR) approaches [9,14], and recently, digital PCR (dPCR) has become widely accepted for its robust and accurate DNA quantification by directly measuring the copy number concentration of target DNA without the aid of external calibration [11,13,15,16]. Although dPCR still requires rigorous optimization and validation for each assay [17], its accuracy and sensitivity is now appreciated in such various areas as liquid biopsy and pathogen detection [18,19]. In addition, results from *in vitro* systems have differed significantly in the identified amount and size between cell lines and conditions [20,21], warranting further studies in comparing and optimizing methods of DNA analysis.

In this study, we report a set of novel dPCR assays for measuring DNA fragmentation from cells exhibiting induced cytotoxic response. First, we establish a cell culture system representing differential degrees of cell death process following anti-cancer drug treatment. This induced cytotoxicity is measured by time-course assays for total cell counts, viability, and annexin V-positive cell percentage, with results then compared with the levels of DNA fragmentation derived from dPCR analysis using both cellular and cell-free DNA as templates. In particular, using the amplicons from RNase P (RP) gene locus [22–24], we suggest here the *RP DNA fragmentation index*, which we define as the ratio of shorter targets to a long target within an overlapping locus. After verifying these assays using untruncated genomic DNA, we show that both cellular and cell-free DNA from human cell lines are increasingly fragmented after anti-cancer drug treatment over time. Ultimately, our study demonstrates a dPCR application for measuring DNA fragmentation that quantitatively reflects the degree of cytotoxicity.

2. Results and discussion

2.1. Cell line-specific responses to the anti-cancer drug camptothecin

In order to obtain human cells undergoing cell death, we induced cytotoxicity by treating four different human cancer cell lines with anti-cancer drugs. First, the chemicals cycloheximide, dexamethasone, etoposide, and camptothecin (CPT) were tested at each recommended concentration on two different colorectal adenocarcinoma cell lines, SW480 and SW620 (Supplementary Fig. 1A). With these two cell lines, 10 μM CPT treatment for 24 or 48 h was found to be the most effective in reducing cell viability and inhibiting cell proliferation (Supplementary Fig. 1A). As our initial aim was to establish cell culture conditions undergoing cell death with differential degrees, we expanded our time points and number of cell lines using CPT at 10 μM for the rest of this study.

In addition to SW480 and SW620, the monocytic leukemia cell line THP-1 and mammary adenocarcinoma cell line MCF7 were also tested with CPT. In each condition, cells were collected for cell counting and viability analysis at three different time points (5, 24, and 48 h), and temporal trends in the cell count fold changes normalized to the seeding cell number were compared (Fig. 1A). In the untreated and dimethyl sulfoxide- (DMSO-) treated controls, all four cell lines exhibited a considerable increase in cell counts over time (Fig. 1A, grey and dotted black lines). These results suggest robust cell proliferation in our control samples, albeit at varying rates reflecting each cell line's distinct proliferative capacity. On the other hand, CPT-treated cells not only failed to proliferate but their viability was noticeably compromised over time (Fig. 1A and B, red lines). Among the four cell lines, THP-1 showed the highest sensitivity to CPT, followed by MCF7. SW480 and SW620 were relatively insensitive to CPT treatment at 10 μM. This differential sensitivity to CPT treatment was also reflected in flow cytometry analyses using annexin V staining (Fig. 1C). THP-1 was highly sensitive to CPT, with > 70% of cells being annexin V positive even after just 5 h of treatment. On the other hand, SW480, SW620, and MCF7 cells were resistive to CPT treatment, although more CPT-treated SW480 and SW620 cells appeared positive following annexin V staining compared to DMSO control samples, while MCF7 cells showed no response.

2.2. Development and validation of digital PCR assays for measuring DNA fragmentation

Next, we tested if properties of DNA isolated from cell pellets (cellular DNA) can be used for measuring levels of cell death. Cellular DNA is often subjected to the conventional DNA laddering assay, which visualizes DNA fragmentation patterns on an electrophoresis gel [3]. Over multiple attempts, the DNA laddering assays were neither consistent nor sensitive enough here to show the expected laddering pattern; only hints of DNA laddering in our samples were occasionally observed in the THP-1 cellular DNA after CPT treatment (Supplementary Fig. 1B). In addition, the time-course cellular DNA concentration itself exhibited no clear correlation with either cell count or viability (Supplementary Fig. 1C). Our results suggest that the DNA laddering assay alone is insufficient to readily assess DNA fragmentation during cytotoxic response.

Alternatively, DNA fragmentation can be measured by qPCR [9,14] or dPCR. As the latter can provide the copy number concentration of the target DNA, we designed a set of dPCR assays to quantify targets of differential sizes within an overlapping genomic region. We first hypothesized that if the template DNA is fragmented, the copy number concentration of smaller DNA targets will be higher than that of larger ones in a given sample. In contrast, if the template DNA is not fragmented (i.e. high molecular weight genomic DNA), the copy number concentrations from any sample will be constant regardless of the size of amplicons, given that a comparable PCR efficiency was first verified.

To test this possibility, we first applied a set of dPCR assays initially designed for multiple genomic regions but narrowed down to the RP gene locus (Fig. 2A). Each set of assays, RP1 and RP2, are designed to amplify regions of incrementally increasing sizes, ranging between 75 and 208 base pairs. After dPCR, we can calculate the ratio of the copy number concentrations of smaller targets to the longest target. For consistency, we named this ratio the *RP fragmentation index*. Theoretically, the RP fragmentation index equals 1 if the template DNA is not fragmented (i.e. high molecular weight genomic DNA), while the index becomes higher than 1 when the shorter amplicons are more abundant than the longest one, thereby indicating template DNA fragmentation. For example, in the first set, an RP1 fragmentation index is defined as a smaller RP1 target concentration divided by RP1(195), which is the longest DNA target in this set. Hence, the fragmentation index RP1(70) indicates a copy number ratio of RP1(70) to RP1(195).

We validated this assay scheme using genomic DNA isolated from MCF7 and THP-1 cells as templates. First, we confirmed that these RP dPCR assays can provide reliable results by examining one-dimensional plots (Fig. 2B). Positive and negative droplets are easily distinguishable in each assay, although the signal amplitudes vary widely between assays (Fig. 2B). The copy number concentrations for each target were measured using the same amount of template DNA (Fig. 2B and C). Using these copy number values, RP1 and RP2 fragmentation indices were calculated for each amplicon. As expected, the indices were essentially one in all cases for both cell lines when genomic DNA was used as the template (Fig. 2D). Such data validate these assays by demonstrating that the amplification efficiencies of each tested dPCR assay were comparable, being independent of amplicon sizes when mostly intact genomic DNA is used as the template. Therefore, we concluded that our RP fragmentation indices derived from dPCR results can effectively measure the level of DNA fragmentation.

2.3. Application of the RP fragmentation index for measuring cytotoxic response

We then asked if the RP fragmentation indices could distinguish cells undergoing cell death process from normal cells. For dPCR

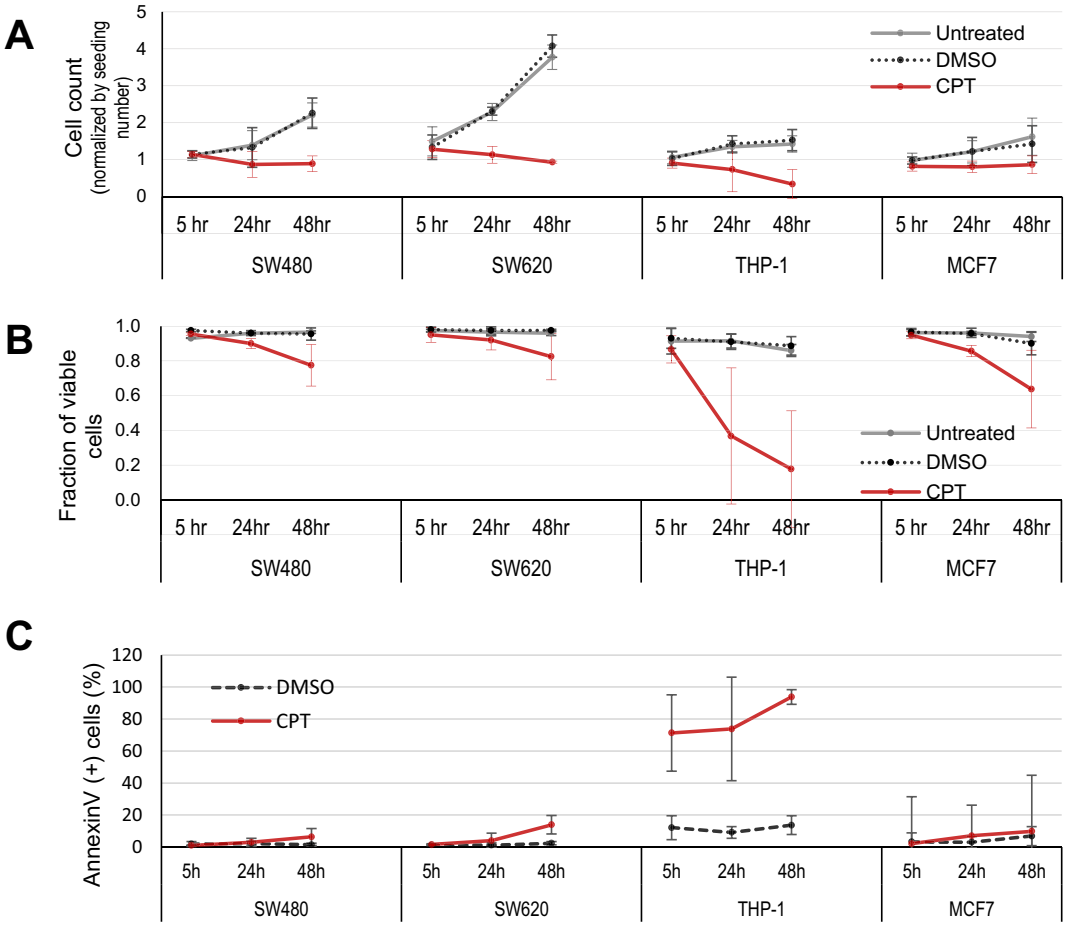

Fig. 1. Cytotoxic response of SW480, SW620, THP-1, and MCF7 cell lines after 10 uM CPT treatment. The grey and dotted lines indicate untreated and DMSO control, respectively. Red lines indicate the CPT-treated samples. (A) Time-course cell numbers normalized to the initial seeding cell counts after corresponding treatment. (B) Time-course cell viability in each indicated condition. (C) Percentage of annexin V-positive cells for each cell line over time. Error bars in each graph indicate the standard deviation of three or more biological replicates.

templates, we used cellular DNA isolated from THP-1 cells treated with CPT (1 or 10 μM) for 2, 5, and 24 h. Each sample of cellular DNA was subjected to dPCR to measure the copy number concentrations of RP amplicons of variable sizes from same amount of template DNA. For DMSO control samples, the RP copy number concentrations did not change as the amplicon length incrementally increased (Fig. 3A and B), recalling the results from the genomic DNA samples (Fig. 2C). Accordingly, the RP fragmentation indices of DMSO-treated controls remained between 0.9 and 1.05, approximately, in both RP1 and RP2 assays (Fig. 3C, black lines). We conclude that DMSO treatment does not elicit DNA fragmentation, at least within the two targeted regions.

Sufficient exposure to CPT causes an increase in the RP fragmentation index. After 2 and 5 h of CPT treatment (10 μM), the RP fragmentation index did not change significantly for RP1(70) and RP2(85) compared to the DMSO control, reaching about 1.1 (Fig. 3C, grey lines). After 24 h of CPT treatment (1 or 10 μM), a negative correlation between copy number concentration and amplicon length became evident (Fig. 3A and B). This incremental reduction in copy number concentration for longer PCR amplicons reflects gradual DNA fragmentation patterns in the template DNA. This trend is again represented in much-elevated RP fragmentation indices for shorter amplicons (Fig. 3C, blue and red lines). Specifically, RP1(70) and RP2(85) indices were significantly raised after 24 h of CPT exposure compared to the DMSO control (Fig. 3C, blue and red asterisks). These combined data suggest that the RP fragmentation indices can detect cellular DNA fragmentation after 24 h of CPT treatment (Fig. 2C, red and blue lines).

As the RP fragmentation indices were much higher for the four shortest sets (RP1(70), RP1(99), RP2(85), and RP2(92)), these assays were selected for further experiments. We isolated cellular DNA after CPT treatment from four cell lines at three different time points (5, 24, and 48 h). The selected four fragmentation indices were calculated based on dPCR results (Fig. 3D). For cellular DNA isolated from SW480, SW620, and MCF7, the four RP fragmentation indices did not change by CPT treatment, maintaining a value between about 0.9 and 1.1 (Fig. 3D). These data indicate that cellular DNA from these cell lines was not fragmented by CPT treatment, at least within the targeted regions. On the other hand, THP-1 cellular DNA exhibited drastic changes in these four RP fragmentation indices, reaching up to 2.3 at 48 h of CPT treatment (Fig. 3D). It is noteworthy that the indices using the two shortest amplicons (RP1(70) and RP2(85)) were higher than the other two from relatively longer amplicons (RP1(99) and RP2(92)). This cell line-specific sensitivity is similarly shown with other analyses, as in Fig. 1 where the THP-1 cell line was the most sensitive to CPT. Based on such results, our combined data suggest that the RP fragmentation indices can effectively measure differential degrees of DNA fragmentation during cytotoxic response.

2.4. Fragmentation in cell-free DNA upon CPT treatment

Extracellular DNA released by cells can be detected in *in vitro* cell culture medium [21]. We hypothesized that cellular response to CPT treatment may be predicted by identifying the nature of these cell-free DNA (cfDNA). We first measured the amount of cfDNA released by THP-1 and MCF7 cells, which showed a relatively high sensitivity to

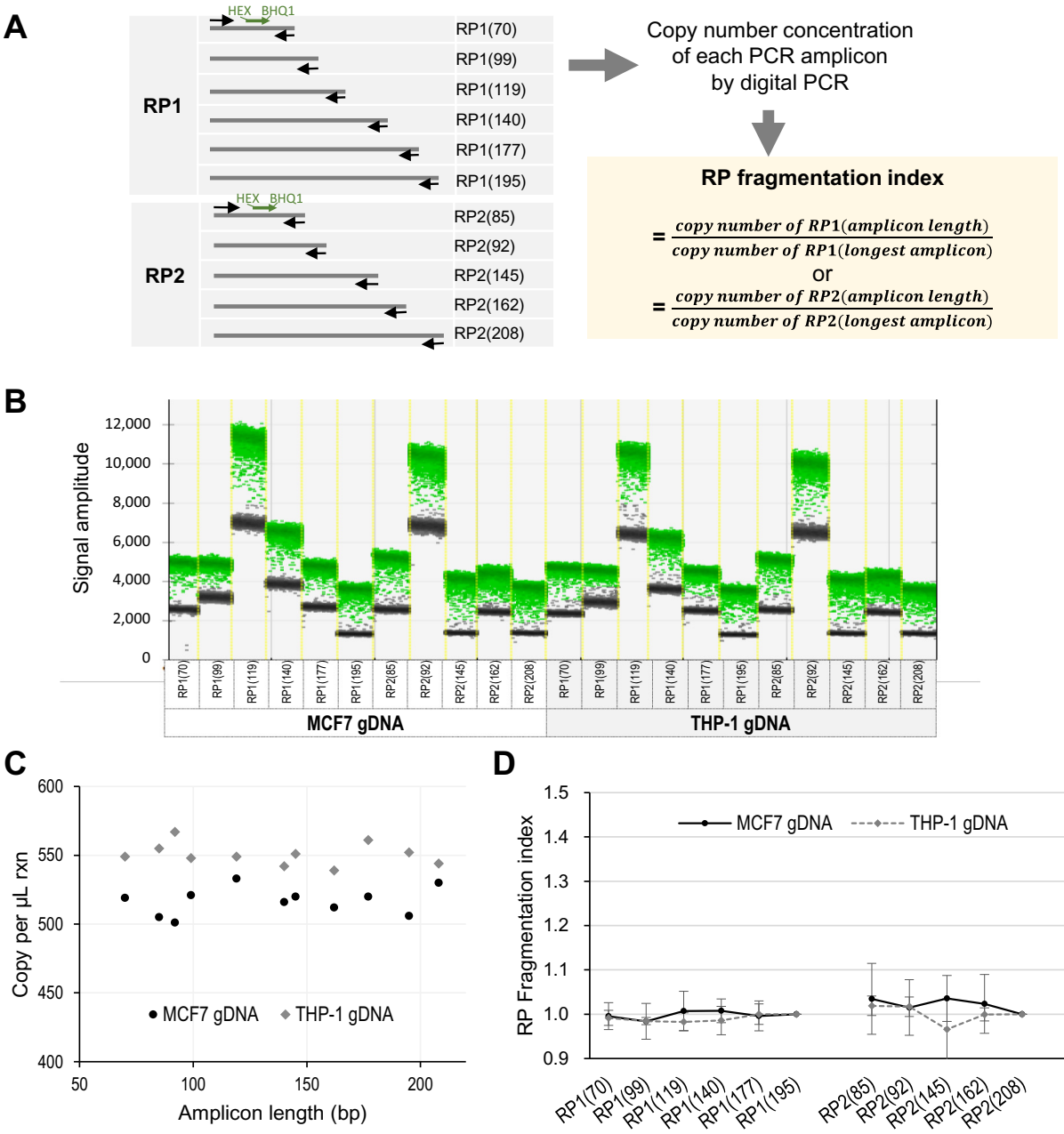

Fig. 2. Validation of digital PCR assays for DNA fragmentation. (A) Experimental schemes for dPCR assays and calculation of RP fragmentation indices. Arrows place the relative positions within the target locus, which incrementally increase as indicated by the number in parentheses. For example, RP1(70) indicates a PCR product of 70 bp in length. The listed six RP1 PCR reactions and five RP2 reactions were applied to each template DNA. Copy number concentrations of each target were used to calculate the ratio of short/long amplicons for each RP1 and RP2 set. The long amplicons used for RP fragmentation indices were RP1(195) and RP2(208) for RP1 and RP2 assays, respectively. (B) Representative one-dimensional plot of a dPCR assay set using genomic DNA from MCF7 and THP-1 cells. For each assay, the positive (green) and negative (grey) droplets are clearly separated. (C) Representative dataset from one biological sample showing copy number concentration (copy per µL reaction) for each genomic DNA template plotted along the amplicon length for both RP1 and RP2 assays. (D) RP fragmentation indices plotted for the results from each indicated dPCR in copy number concentration from (C) divided by either RP1(195) or RP2(208) concentration. Untruncated genomic DNA isolated from MCF7 and THP-1 cells was used as template DNA. Error bars in the graph indicate the standard deviation of three or more biological replicates.

CPT in cell viability (Fig. 1). The cfDNA amount appeared to neither positively nor negatively correlate with the viability or total cell number of the culture (Figs. 1 and 4A). Although this may be partially due to an incomplete and variable DNA extraction efficiency, our data suggest that the cfDNA amount itself is not a dependable indicator of cell death.

In vivo studies have found that circulating cfDNA is produced by apoptosis with size profiles reflecting nucleosomal units of approximately 165 bp [25]; we then asked if cfDNA isolated in *in vitro* culture also carries similar properties. To answer this, we measured the fragmentation index of RP2(85) with only the limited amount of cfDNA available for multiple dPCR assays. Unlike cellular DNA following DMSO treatment, we found that both THP-1 and MCF7 cfDNA isolated from control culture media (DMSO or untreated) were highly fragmented, showing RP fragmentation indices of over four (Fig. 4B). These data suggest truncated cfDNA is released spontaneously even without CPT treatment.

Time-course analyses of CPT-induced cfDNA fragmentation in THP-1 and MCF7 cells exhibited distinct patterns. The cfDNA originating from THP-1 did not show any significant changes in RP fragmentation

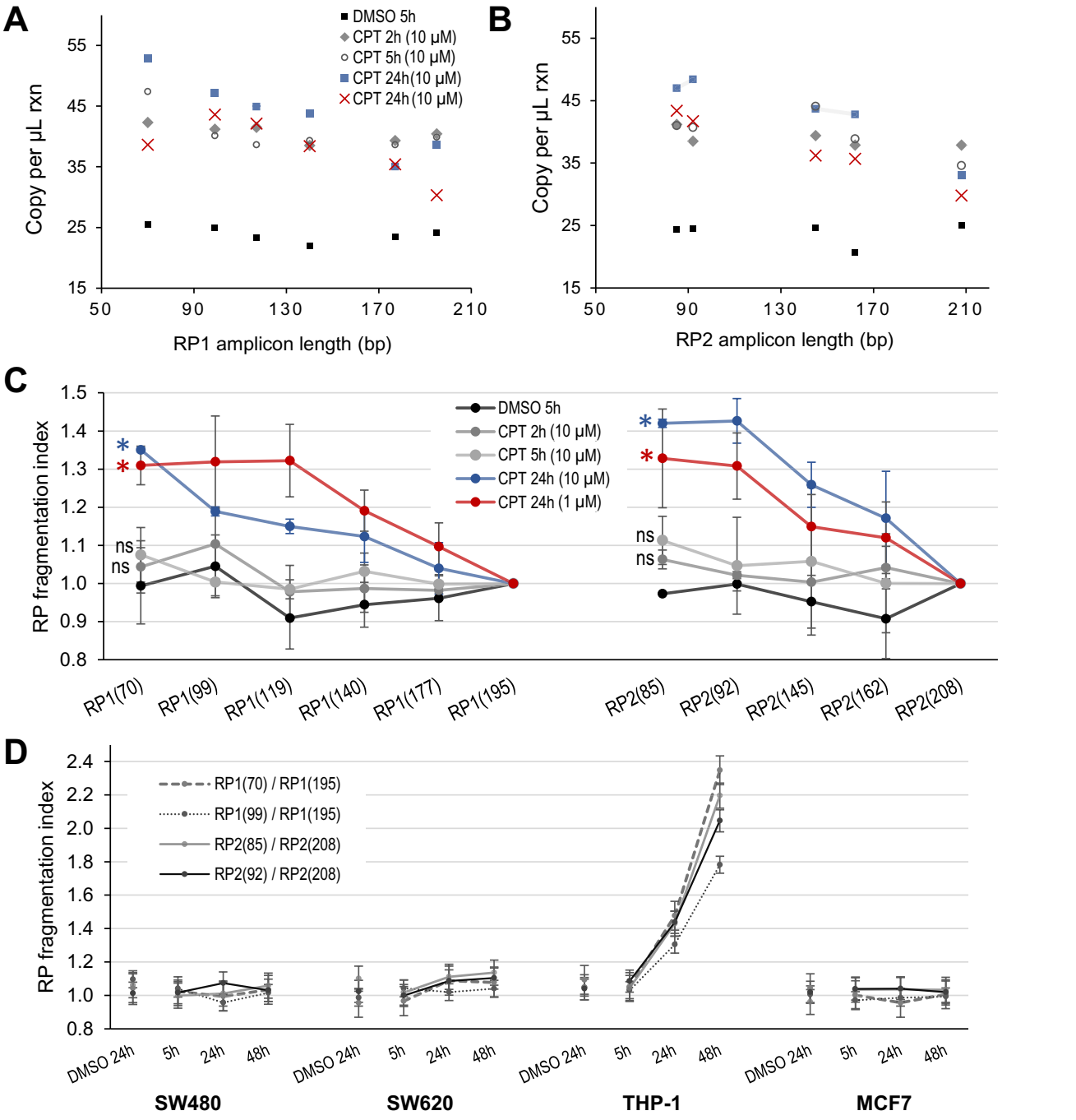

Fig. 3. Application of dPCR assays and RP fragmentation index to cellular DNA. (A–B) Representative copy number concentration dataset from one biological sample of THP-1 cellular DNA isolated after indicated treatment conditions. The *x*-axis indicates the length of each RP assay and the *y*-axis indicates the copy number concentration of the targeted amplicon. (A) Copy number concentrations of RP1 amplicons. (B) Copy number concentrations of RP2 amplicons. (C) RP fragmentation indices calculated based on copy number concentrations from multiple biological replicates from the cellular DNA of THP-1 cells after CPT treatment as template DNA. Each asterisk indicates a significant increase (p-value < 0.05) compared to DMSO control, while 'ns' indicates a 'not significant' increase compared to control. (D) Comparison of time-course trends of four selected RP fragmentation indices (RP1(70)/RP1(195), RP1(99)/RP1(195), RP2(85)/RP2(208), and RP2(92)/RP2(208)) using cellular DNA isolated from each indicated cell line. DMSO-treated samples were included for each set of cell lines along with 10 µM CPT treatment for 5, 24, and 48 h. Error bars in each graph indicate the standard deviation of three or more biological replicates.

index after CPT treatment, maintaining a value similar to untreated and DMSO controls (Fig. 4B). On the other hand, the RP fragmentation index of MCF7 cfDNA steadily increased over time (Fig. 4B); at 48 h of CPT treatment, the average RP2(85) fragmentation index was about 25, indicating a high level of DNA fragmentation. It is noteworthy that these index values of MCF7 cfDNA after 24 and 48 h of CPT treatment are probably underestimated, because more than one dataset failed to detect the long target (RP2(208) amplicon), impeding calculation of the ratio (giving a zero denominator). Otherwise, the copy number of the short target (RP2(85)) was abundant (data not shown). These data indicate a high level of DNA fragmentation within the targeted region in cfDNA secreted from MCF7 but not from THP-1. The discrepancy in RP fragmentation indices between cellular DNA and cfDNA from MCF7 and THP-1 may possibly stem from distinct nucleosomal positioning

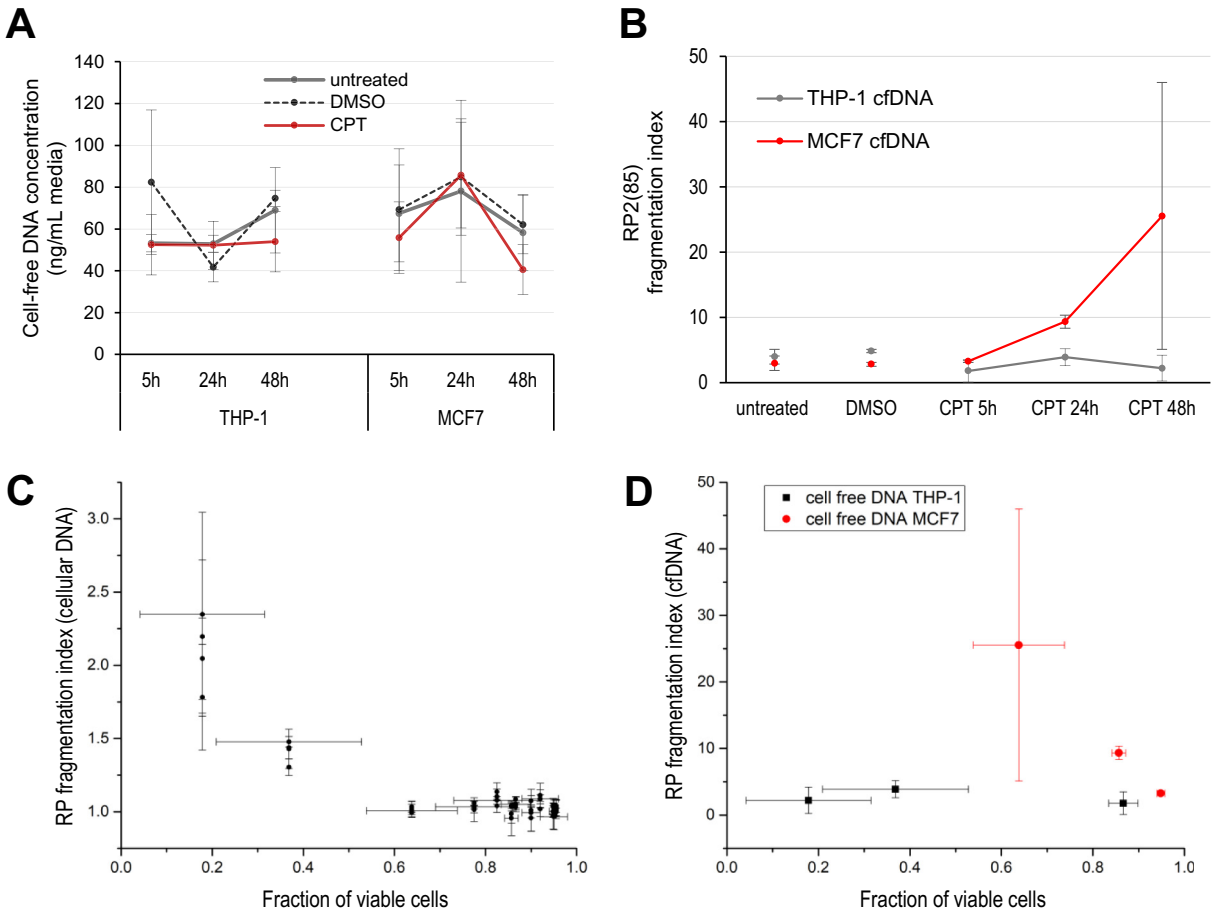

Fig. 4. Analyses of RP fragmentation indices using cell-free DNA isolated from THP-1 and MCF7 cell culture media. (A) Concentration of cfDNA at each time point after 10 μM CPT-treated (red), DMSO-treated (dashed), and untreated (grey) cultures. Error bars indicate the standard deviation from three biological replicates. (B) Changes in the RP2(85) fragmentation index in cfDNA from either THP-1 or MCF7 culture. Error bars indicate the standard deviation from two or more biological replicates. (C) Scatter plot of four RP indices derived from cellular DNA of the four cell lines (Fig. 3D) against the fraction of viable cells of each cell line at matching time points. (D) Scatter plot of RP2(85) indices derived from the cfDNA of indicated cell lines plotted against the fraction of viable cells.

reflected in a specific truncation pattern of cfDNA.

The RP fragmentation indices from cellular DNA and cfDNA exhibited a negative correlation with cell viability in some cases. To evaluate if our RP fragmentation index can potentially assess cell viability, we generated scatter plots (Fig. 4D and D) to show the trend of the fraction of viable cells (Fig. 1B) relative to their RP fragmentation indices (Fig. 3D). Especially for cellular DNA, combined results from the four cell lines exhibited a general negative correlation (Fig. 4C). On the other hand, RP fragmentation indices from cfDNA showed clear cell-line specificity, where the RP fragmentation index from only MCF7-originated cfDNA, but not THP-1, was negatively correlated with cell viability.

3. Conclusions

In this study, we demonstrated the validity of specific dPCR assays for the quantitative assessment of DNA fragmentation due to cytotoxic response. Results from dPCR assays are converted to a copy number ratio of a short amplicon over that of the longest amplicon, producing RP fragmentation indices. Analogous approaches have been applied to plasma DNA and DNA extracted from fixed tissue [11,13]. This current study demonstrates that cytotoxic response induces DNA fragmentation, the degree of which is differentially reflected in the RP fragmentation indices. The sensitivity of the RP fragmentation indices in detecting the degree of cell death process is at least comparable to conventional cytometric assays, although this needs to be systematically explored in the future. Our dPCR assays also exhibited the capability to detect differential DNA fragmentation statuses of cfDNA, which were distinctively cell-type specific compared to the results from cellular DNA. We note that the choice of DNA extraction method can generally affect the size distribution of DNA, possibly limiting the utility of this assay. Nonetheless, our medium-originated cfDNA analyses using dPCR assays present the potential to measure DNA fragmentation as a cytotoxic response without harvesting cultured cells, a feature unachievable with any existing cytometric assay. We envision that the assay developed here could provide for precise and sensitive time-course measurement of DNA fragmentation induced by cytotoxic response. The addition of other reference genes to this dPCR assay by multiplexing would highly benefit its general utility and possibly overcome the observed cell-type specificity of this method.

4. Materials and methods

4.1. Cell lines and culture

SW480, SW620, and THP-1 cells (ATCC) were grown in RPMI-1640 media containing 10% FBS and 1% penicillin/streptomycin. MCF7 cells (ATCC) were grown in DMEM media containing 10% FBS and 1% penicillin/streptomycin. The cells were incubated at 37 °C in a humidified chamber at 5% CO_2. All culture supplies were obtained from Thermo Fisher Scientific unless otherwise indicated.

4.2. Induction of cell death

SW480, SW620, THP-1, and MCF7 cells were seeded in 6-well plates (2×10^6 cells per well) or 100 mm dishes (8×10^6 cells per dish). The cells were grown for 16 h and then the culture media was changed to media containing either DMSO or cell death-inducing chemicals, such as cycloheximide (100 μM), dexamethason (10 μM), etoposide (10 μM), and camptothecin (10 μM) (Millipore). After exposure to each chemical, cells were harvested at different time points (5, 12, 24, and 48 h) and the cell count was obtained by an automated cell counter (Countess). The cell count and viability were measured twice and then average values were assigned.

4.3. Annexin V by flow cytometry

Cells were harvested and diluted to match the concentration of 10^6 cells/mL. Cell pellets were washed twice in 1× PBS and re-suspended in 1 mL binding buffer (BioLegend). For staining, 5 μL of Annexin V-FITC (Invitrogen) was added to 100 μL of cell suspension, which was then incubated in the dark for 15 min and then re-suspended in 400 μL of binding buffer. The cells were analyzed using a FACSVerse (BD Biosciences). Data was exported in FCS file format and analyzed using FlowJo (version X10, FlowJo LLC). Experiments were independently repeated at least in triplicate. Error bars in the graphical data represent standard deviations.

4.4. DNA Extraction and quantification

Cellular DNA was extracted from cells cultured in a 6-well plate after chemical exposure using the Apoptotic DNA Ladder kit (Roche) according to the manufacturer's instruction. The final elution volume was 100 μL. Cell-free DNA was extracted from cells cultured in a 100 mm dish. After chemical treatment, 10 mL of the culture medium was collected in a 15 mL conical tube and then centrifuged at 100 ×*g* for 10 min. The supernatant was transferred to a new 15 mL conical tube. Two additional centrifugations were subsequently carried out: 1000 ×*g* for 10 min, and 10,000 ×*g* for 30 min. From the resulting 9 mL of media, cfDNA was extracted using a QIAamp Circulating Nucleic Acid kit (QIAGEN) according to the manufacturer's instruction. The cfDNA was eluted with 10 μL AVE buffer. In order to obtain high molecular weight DNA, genomic DNA was extracted from MCF7 and THP-1 cells. For this, 1×10^6 cells were seeded in a 6-well plate and incubated for 16 h. The harvested cells were washed twice with 1× PBS. DNA was extracted according to guidelines using a Blood & Cell Culture DNA Midi Kit (QIAGEN). The amount of DNA was quantified with Nanodrop (Thermo Fisher Scientific).

4.5. Digital PCR assays

Each RP1 and RP2 assay shares forward primers and positions the reverse primers differently. The sequence of primers for RP1 forward was 5′- GGGAGTGTTGGAACAATACTATCTA-3′. The sequences of the reverse primers were as follows: RP1(70): 5′- ACTCCGCTGTGTATGTC CTC-3′; RP1(99): 5'-TTGGGCCATGCTATCCTC-3′; RP1(119): 5′- CTTT CGCTTCCCTTCGAT -3′; RP1(140): 5'-ACAGGTTCTCGTCTCTCA AGG-3′; RP1(177): 5'-CGGAATACAGAACCCATGAC-3′; and RP1(195): 5′- CCAACACTTTACAGTCTACGGAAT-3′. The RP1 hybridization probe was 5' HEX-AGAGGACATACACAGCGGAGTG-BHQ1 3′. The sequence of primers for RP2 forward was 5'-GATGGGTCTCGGTCAGGT-3′. The sequences of the reverse primers were as follows: RP2(85): 5′- GCGCTA GGAATCAGACCA-3′; RP2(92) 5'-GAGTTTCCCGCGCTAGG-3′; RP2(145): 5′- TCCCTCATTGCAGGAAAGTA-3′; RP2(162): 5'-CCTCGTT AGGCCTCAGTTC-3′; and RP2(208): 5'-GGCTTCTGTCACCTATCAGC-3′. The RP2 hybridization probe was 5' HEX-CAGAGTCTCTGGGATGTC CCT-BHQ1 3′.

The PCR reaction mixture consisted of a template DNA, 0.2 μmol/L of the forward and reverse primers, and 10 μL of 2× ddPCR Supermix for Probes (Bio-Rad) for a total reaction volume of 20 μL. After droplet generation using a QX200 generator, PCR was performed in a 96-well plate using an ABI StepOnePlus thermal cycler. Thermal cycling conditions were as follows: 95 °C for 5 min, 40 cycles (ramp rate reduced to 30% of the maximum, approximately 2.5 °C/s) of denaturation at 95 °C for 30 s, annealing and extension at 58 °C for 1 min, and droplet stabilization at 98 °C for 10 min. A no-template control (NTC) was included in every assay to separate the positive and negative droplets. For each set of reactions, an equal amount of template DNA was first added to the master mix solution, which was divided equally to each preparation, ensuring that target DNA copy number measurements between samples were drawn from the same amount of template DNA. dPCR data were analyzed with QuantaSoft 1.7.4 using mostly default settings, except for the thresholds which were set manually based on the NTC controls. For statistical analyses, one-tailed *t*-tests assuming unequal variances were conducted.

Author contributions

J.-R.H., Y.-K·B. and J.Y. L. designed the experiments and conducted experiments. Y.-K.B. and J.Y. L. analyzed the data. J.-R.H. and Y.-K.B wrote the paper.

Acknowledgements

This research was supported by KRISS (GP2019-0009-01) and KRISS (GP2019-0006-02).

Appendix A. Supplementary data

Supplementary data to this article can be found online at https://doi.org/10.1016/j.bbagen.2019.05.001.

References

[1] L. Galluzzi, et al., Molecular mechanisms of cell death: recommendations of the nomenclature committee on cell death 2018, Cell Death Differ. 25 (3) (Mar. 2018) 486–541.
[2] A. Ashkenazi, G. Salvesen, Regulated cell death: Signaling and mechanisms, Annu. Rev. Cell Dev. Biol. 30 (1) (Oct. 2014) 337–356.
[3] G. Banfalvi, Methods to detect apoptotic cell death, Apoptosis 22 (2) (Feb. 2017) 306–323.
[4] A.H. Wyllie, Glucocorticoid-induced thymocyte apoptosis is associated with endogenous endonuclease activation, Nature 284 (5756) (Apr. 1980) 555–556.
[5] M.B. Giacona, G.C. Ruben, K.A. Iczkowski, T.B. Roos, D.M. Porter, G.D. Sorenson, Cell-free DNA in human blood plasma: length measurements in patients with pancreatic cancer and healthy controls, Pancreas 17 (1) (Jul. 1998) 89–97.
[6] P. Jiang, Y.M.D. Lo, The long and short of circulating cell-free DNA and the ins and outs of molecular diagnostics, Trends Genet. 32 (6) (Jun. 2016) 360–371.
[7] C. Bettegowda, et al., Detection of circulating tumor DNA in early- and late-stage human malignancies, Sci. Transl. Med. 6 (224) (Feb. 2014) 224ra24.
[8] H. Schwarzenbach, D.S.B. Hoon, K. Pantel, Cell-free nucleic acids as biomarkers in cancer patients, Nat. Rev. Cancer 11 (6) (Jun. 2011) 426–437.
[9] F. Mouliere, et al., High fragmentation characterizes tumour-derived circulating DNA, PLoS ONE 6 (9) (Sep. 2011) e23418.
[10] N. Umetani, et al., Increased integrity of free circulating DNA in sera of patients with colorectal or periampullary cancer: direct quantitative PCR for ALU repeats, Clin. Chem. 52 (6) (Jun. 2006) 1062–1069.
[11] M.R. Fernando, C. Jiang, G.D. Krzyzanowski, W.L. Ryan, Analysis of human blood plasma cell-free DNA fragment size distribution using EvaGreen chemistry based droplet digital PCR assays, Clin. Chim. Acta 483 (Aug. 2018) 39–47.
[12] K.C.A. Chan, et al., Size distributions of maternal and Fetal DNA in maternal plasma, Clin. Chem. 50 (1) (Jan. 2004) 88–92.
[13] A. Didelot, et al., Multiplex Picoliter-droplet digital PCR for quantitative assessment of DNA integrity in clinical samples, Clin. Chem. 59 (5) (May 2013) 815–823.
[14] Y.-J. Gao, et al., Increased integrity of circulating cell-free DNA in plasma of patients with acute leukemia, Clin. Chem. Lab. Med. 48 (11) (Jan. 2010) 1651–1656.
[15] A.S. Whale, et al., Assessment of digital PCR as a primary reference measurement procedure to support advances in precision medicine, Clin. Chem. 64 (9) (Sep. 2018) 1296–1307.
[16] A.S. Whale, A. Fernandez-Gonzalez, A. Gutteridge, A.S. Devonshire, Control materials and digital PCR methods for evaluation of circulating cell-free DNA extractions from plasma, *Methods in molecular biology (Clifton, N.J.)*, Vol. 1768, 2018, pp. 45–65.

[17] J.F. Huggett, et al., The digital MIQE guidelines: minimum information for publication of quantitative digital PCR experiments, Clin. Chem. 59 (6) (Jun. 2013) 892–902.
[18] I. Gutiérrez-Aguirre, N. Rački, T. Dreo, M. Ravnikar, Droplet digital PCR for absolute quantification of pathogens, *Methods in molecular biology (Clifton, N.J.)*, Vol. 1302, 2015, pp. 331–347.
[19] C.M. Hindson, et al., Absolute quantification by droplet digital PCR versus analog real-time PCR, Nat. Methods 10 (10) (Oct. 2013) 1003–1005.
[20] J. Aucamp, A.J. Bronkhorst, D.L. Peters, H.C. Van Dyk, F.H. Van der Westhuizen, P.J. Pretorius, Kinetic analysis, size profiling, and bioenergetic association of DNA released by selected cell lines in vitro, Cell. Mol. Life Sci. 74 (14) (Jul. 2017) 2689–2707.
[21] A.J. Bronkhorst, J.F. Wentzel, J. Aucamp, E. van Dyk, L. du Plessis, P.J. Pretorius, Characterization of the cell-free DNA released by cultured cancer cells, Biochim. Biophys. Acta, Mol. Cell Res. 1863 (1) (Jan. 2016) 157–165.
[22] S. Ota, et al., Quantitative analysis of viral load per haploid genome revealed the different biological features of Merkel cell Polyomavirus infection in skin tumor, PLoS ONE 7 (6) (Jun. 2012) e39954.
[23] A.S. Whale, et al., Comparison of microfluidic digital PCR and conventional quantitative PCR for measuring copy number variation, Nucleic Acids Res. 40 (11) (Jun. 2012) e82.
[24] Q. Zhong, et al., Multiplex digital PCR: breaking the one target per color barrier of quantitative PCR, Lab Chip 11 (13) (Jun. 2011) 2167.
[25] P.O. Delgado, et al., Characterization of cell-free circulating DNA in plasma in patients with prostate cancer, Tumor Biol. 34 (2) (Apr. 2013) 983–986.